Scanning Electrochemical Microscopy. 49. Gas-Phase Scanning Electrochemical Microscopy Measurements with a Clark Oxygen Ultramicroelectrode

Maurizio Carano, Katherine B. Holt, and Allen J. Bard*

Department of Chemistry and Biochemistry, The University of Texas at Austin, Austin, Texas 78712

The use of an ultramicroelectrode tip as a basis for a Clark membrane electrode allows the sensing of oxygen concentration using the oxygen reduction signal and the application of scanning electrochemical microscopy (SECM) to pure gas-phase measurements. A 25-μm-diameter Pt wire was sealed in glass and the glass coated with silver paint near the tip to produce a Ag ring, Pt disk electrode. A drop of electrolyte provided the contact between the Pt cathode indicator electrode and the Ag anode counter/reference electrode, while the liquid phase was maintained by a high-density polyethylene membrane pulled over the tip and fastened with an O-ring. The membrane isolated the electrode both electrically and chemically from the sample environment. The electrode was tested with both solution- and gas-phase samples, and SECM approach curves were recorded. The presence of a membrane caused a deviation in electrode behavior from theory in both solution and gas phases, due in part to an increase in the electrode response time. However, the approach curves obtained could be used to determine the distance of the membrane from a surface and the thickness of the electrolyte layer within the membrane. SECM images in the gas phase, of oxygen flux through an array of 100-μm-diameter holes in a silicon wafer, were obtained by measuring the reduction current of oxygen while scanning in the $x-y$ plane over the surface.

Electrochemical methods have been used extensively for the measurement of oxygen concentration and flux. In principle, it is possible to use many electrode systems to detect oxygen.[1] The problems of interference by other electroactive species or the poisoning of the sensing electrode surface by impurities was largely solved by covering the electrode surface with a membrane that allows the passage of oxygen but not other solution species and minimizes changes in the electrolytic composition over time.[2,3] A unique characteristic of a membrane-covered electrode is that the membrane provides a finite diffusion layer of controlled thickness to the electrode. Moreover, by placing both the working and counter/reference electrodes behind the membrane that immobilizes the electrolyte, measurements in the gas phase are possible. These Clark electrodes have been widely used for many applications.[4] This paper addresses the use of a Clark-type ultramicroelectrode tip for application in scanning electrochemical microscopy (SECM).

The Clark electrode has a thin membrane, e.g., polyethylene or Teflon, covering a layer of electrolyte and two metallic electrodes. Oxygen diffuses through the membrane and is electrochemically reduced at the cathode. The potential between the cathode and anode is adjusted so that only oxygen is reduced. The greater the oxygen partial pressure, the greater the oxygen flux through the membrane, so that the current is proportional to the oxygen in the sample.

There have been several papers that have dealt with oxygen sensing in SECM, but all of these have used bare Pt or C tips.[5,6] The goal of the present work was to couple SECM with a Clark-type electrode based on a 25-μm-diameter ultramicroelectrode (UME) tip for use either in solution or in the gas phase. By combining the features of SECM[5−7] with the selectivity of the membrane electrode to oxygen, one can envision interesting applications in the study of membranes and biological samples.[8−12] In designing an electrode that can be used as a SECM tip, it was necessary to consider the shape and the RG value (the ratio of the overall radius of the tip and the radius of the platinum disk) of the tip, so that one could move and position the tip close to the sample to collect useful data without the edge of the tip or the

---

* Corresponding author. E-mail: ajbard@mail.utexas.edu.

(1) Hitchman, M. L. In *Measurement of Dissolved Oxygen*; Elving, P. J., Winefordner, J. D., Eds.; Kolthoff, I. M., Ed. Emeritus; John Wiley & Sons: New York, 1978.

(2) Clark, L. C. *T Am. Soc. Art. Int. Org.* **1956**, *2*, 41.

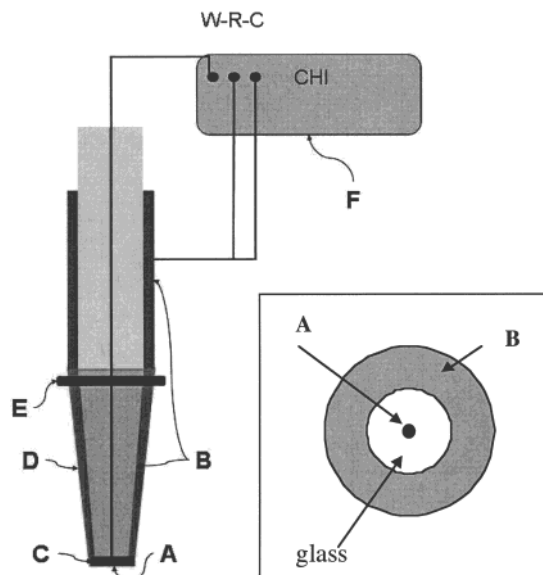(3) Clark, L. C. Electrochemical device for chemical analysis. U.S. Patent 2,-913,386, issued 17 November 1959.

(4) Irving, F. *The polarographic oxygen sensor: its theory of operation and its application in biology, medicine, and technology*; CRC Press: Cleveland, OH, 1976 pp 265−274.

(5) Lee, C.; Kwak, J.; Bard, A. J. *Proc. Natl. Acad. Sci. U.S.A.* **1990**, *87*, 1740.

(6) Horrocks, B. R.; Wittstock, G. In *Scanning Electrochemical Microscopy*; Bard, A. J., Mirkin, M. V., Eds.; Marcel Dekker: New York, 2001; Chapter 11, p 445.

(7) Bard, A. J.; Fan, F. R. F.; Kwak, J.; Lev. O. *Anal. Chem.* **1989**, *61*, 132.

(8) Bu, H.-Z.; Mikkelsen, S.; English, A. *Anal. Chem.* **1995**, *67*, 4071.

(9) Shiku, H.; Shiraishi, T.; Ohya, H.; Matsue, T.; Abe, H.; Hoshi, H.; Kobayashi, M. *Anal. Chem.* **2001**, *73*, 3751.

(10) Ortsater, H.; Liss, P.; Lund, P. E.; Akerman, K. E.; Bergsten, P. *Diabetologia* **2000**, *43*(10), 1313.

(11) Ortsater, H.; Liss, P.; Lund, P. E.; Akerman, K. E.; Bergsten, P. *Adv. Exp. Med. Biol.* **1999**, *471*, 367.

(12) Carlsson, P. O.; Liss, P.; Andersson, A.; Jansson, L. *Diabetes* **1998**, *47*(7), 1027.

Figure 1. Schematic diagram of membrane ultramicroelectrode-based oxygen sensor (not to scale): (A) 25-μm-diameter disk Pt working electrode encased in glass, (B) Ag layer acting as reference/counter electrode, (C) electrolyte film of 0.1 M pH 7 PBS aqueous solution forming the electrolytic contact between working and reference electrodes, (D) 10-μm-thickness HDPE membrane, (E) rubber O-ring, and (F) power supply and electronic instrument for the measurements of the current output. Inset: bottom view of electrode surface (A) 25-μm-Pt disk working electrode encased in glass and (B) Ag paint creating a ring reference/counter electrode.

membrane touching the sample. Moreover, measurements in the gas phase can be complicated by convection problems. SECM measurements in solution all are based on diffusion being the sole or predominant means of mass transfer. The gas phase is less predictable because convective processes occur much more easily due to the much smaller viscosity of the phase. One is also dealing with diffusion coefficients that are orders of magnitude larger than those in solution.

EXPERIMENTAL SECTION

Chemicals and Materials. All chemicals were reagent grade and were used as received. All solutions were prepared with deionized water (Milli-Q, Millipore Corp.). The 10-μm-thick high-density polyethylene (HDPE), obtained from a supermarket, was used as a selective membrane for oxygen detection. GC Electronics silver paint was used as the material for the silver reference electrode.

Fabrication of the SECM UME Oxygen Sensor. Figure 1 shows a schematic diagram of the 25-μm Pt tip sensor used for the SECM experiments. A platinum wire (25-μm diameter, Goodfellow, Cambridge, U.K.) sealed in glass was used to construct the UME tip by the procedure described elsewhere,[13,14] and formed the basis of the oxygen sensor. The edge of the tip was sharpened with sand paper of different roughnesses to reduce the RG to a value of 3−4. At the same time it was necessary that edges of the glass surrounding the Pt disk were not too sharp to

facilitate stretching the polyethylene membrane tight against the electrode surface without tearing. After the tip was polished, a layer of silver paint was applied to the external glass surface up to about two-thirds of the length of the electrode. The electrode was heated in an oven at 110 °C for 1 h to evaporate the solvent present in the silver paint solution. This Ag metal surface was used as the reference/counter electrode in the sensor, and a Cu wire in contact with this part of the electrode allowed an external connection to be established. The Pt disk was carefully cleaned to remove any silver paint that might have contacted it and was polished successively with 1.0-, 0.3-, and 0.05-μm alumina. By checking the surface under a microscope it was possible to verify both the success of the operation and the status of the platinum disk, which must be cleaned well to give good electrochemistry.

Membranes. Two types of membranes are typically used for Clark electrodes, loose membranes and membrane cap assemblies. Loose membranes, as used in this study, are less expensive but are more difficult to install and result in lower precision because the stretching of the membrane and the thickness of the electrolyte layer adjacent to the cathode is less reproducible. However, it was not possible to find commercially available caps that would fit the small dimension of the UME tip. By pulling a loose membrane against the electrode surface and using an O-ring to keep it in position, we obtained reasonable reproducibility in the measurements. Typically, a piece of HDPE membrane of thickness 10 μm (generally of dimensions 30 × 30 mm) was cut, and a drop ($\sim 0.5-1$ μL) of electrolyte (typically 0.1 M, pH 7 phosphate buffer solution (PBS)) was then dropped on the HDPE and brought into contact with the edge of the electrode. The membrane was then pulled tight, carefully ensuring that it did not tear, and secured in place with an O-ring. The electrolyte solution provided the electrolytic contact between working and reference electrode.

Electrolyte. Many electrolytes have been used in membrane oxygen electrodes (e.g., KCl, NaCl, $NaHCO_3$, and KOH),[15] and the relative merits of each has been discussed in the literature. The most important factor for oxygen electrode operation is that a stable steady-state current is obtained in the potential region for oxygen reduction. As the hydroxide ion is the product of the 4-electron reduction of oxygen, there will be a localized increase in pH at the electrode surface during use, which causes a shift in the reduction potential of oxygen to more negative values. In unbuffered solutions, this can result in voltammograms exhibiting an ill-defined region of oxygen reduction and no steady-state limiting current. For this reason, 0.1 M pH 7 PBS was used as electrolyte for most of this work and was replaced periodically. The time the electrolyte lasts for repeated measurements depends on the rate at which oxygen is reduced. Probes with a very small diameter cathode, as in our case, will typically produce currents at the nanoampere level, resulting in a long electrolyte life with the available reservoir volume in comparison with Clarke electrodes with a similar electrolyte layer thickness but with more conventional cathode diameters. In all the measurements, the membrane and the electrolytic solution were changed at least every 5 h.

(13) Bard, A. J.; Fan, F.-R. F.; Mirkin, M. V. In *Electroanalytical Chemistry*; Bard, A. J., Ed.; Marcel Dekker: New York, 1994; Vol. 18, pp 243−373.

(14) *Scanning Electrochemical Microscopy*; Bard, A. J., Mirkin, M. V., Eds.; Marcel Dekker: New York, 2001.

(15) *Measurement of Oxygen by Membrane-Covered Probes*; Linek, J.; Vacek, V.; Sinkule, J.; Benes, P.; Ellis Horwood Series in Analytical Chemistry; Ellis Horwood; New York: 1988 (translation Ed., R. A. Chalmers).

The use of 0.1 M KOH as an electrolyte was explored, and although steady-state limiting currents were obtained for oxygen reduction, there were problems due to rapid deactivation of the electrode surface, so the pH 7 PBS was preferred. Deactivation of the Pt electrode during oxygen reduction at an SECM tip has been discussed recently[16] and the minimization of this effect by potential programming of the tip described. Therefore, before use, our electrode was activated electrochemically by cycling between − 0.35 and 1.2 V until reproducible voltammograms were obtained. This was found to increase the stability of the voltammetric and chronoamperometric response.

The electrolyte layer was reduced to the smallest possible thickness determined by the roughness of the cathode surface and stretching of the membrane. However, it is important that this layer not be too thin, so that the removal of hydroxide ions, the product of the reduction of oxygen in water, from the cathode is still efficient. Experiments employing a thin layer of 1 mM ferrocenemethanol (Aldrich) as the electrolyte solution allowed an estimate of electrolyte film thickness in the range of 20−60 μm, as described further below.

Electrochemical Measurements. A CHI 900 SECM (CH Instruments, Austin, TX) was used for all experiments. Cyclic voltammetry and SECM approach curves were carried out in the gas and liquid phases, and SECM scan imaging experiments were performed in the gas phase. A glass microscope slide was used as a nonconducting surface for approach curves. Approach curves were recorded at tip scan speeds between 0.1 and 10 μm s^{-1}. A silicon wafer (100-μm thickness) with an array of six square holes (100-μm dimension) arranged 400 μm apart in a 2 × 3 array was used for the SECM imaging scan. This array was taped to a Teflon support and screwed to the SECM stage. A hole in the support allowed oxygen (or other gases) to flow through the six holes in the silicon. All experiments were carried out at room temperature.

RESULTS AND DISCUSSION
Cyclic Voltammetric Behavior of the Electrode. The behavior of the Pt disk, Ag ring UME (without a membrane) was tested in an air-saturated aqueous 1 mM ferrocenemethanol solution, with 0.1 M NaCl as the supporting electrolyte. Figure 2a shows the CV obtained for the oxidation of the ferrocenemethanol, exhibiting a limiting current at 0.4 V versus Ag consistent with that predicted for the steady-state current for this species at a 25-μm disk UME. On cycling to negative potentials, a reduction current is obtained, starting at −0.25 V, which rises to a value of ~10 nA at −0.75 V versus Ag. This value is consistent with the steady-state current predicted for the 4-electron reduction of oxygen at a 25-μm disk electrode, at an oxygen concentration in solution of 8.6 mg L^{-1} (expected oxygen concentration in solution at 1 atm pressure in dry air) with $D_s = 2 \times 10^{-5}$ cm^2 s^{-1}. However, the CV clearly shows no steady-state limiting current for oxygen reduction, and the cathodic current continues to rise until the onset of water reduction. This poorly defined limiting diffusion current region for oxygen reduction is probably caused by the localized increase in pH at the electrode surface due to the production of hydroxide ions during oxygen reduction, which shifts the onset of oxygen reduction to more negative potentials and prevents equilibrium from being attained in the unbuffered electrolyte.
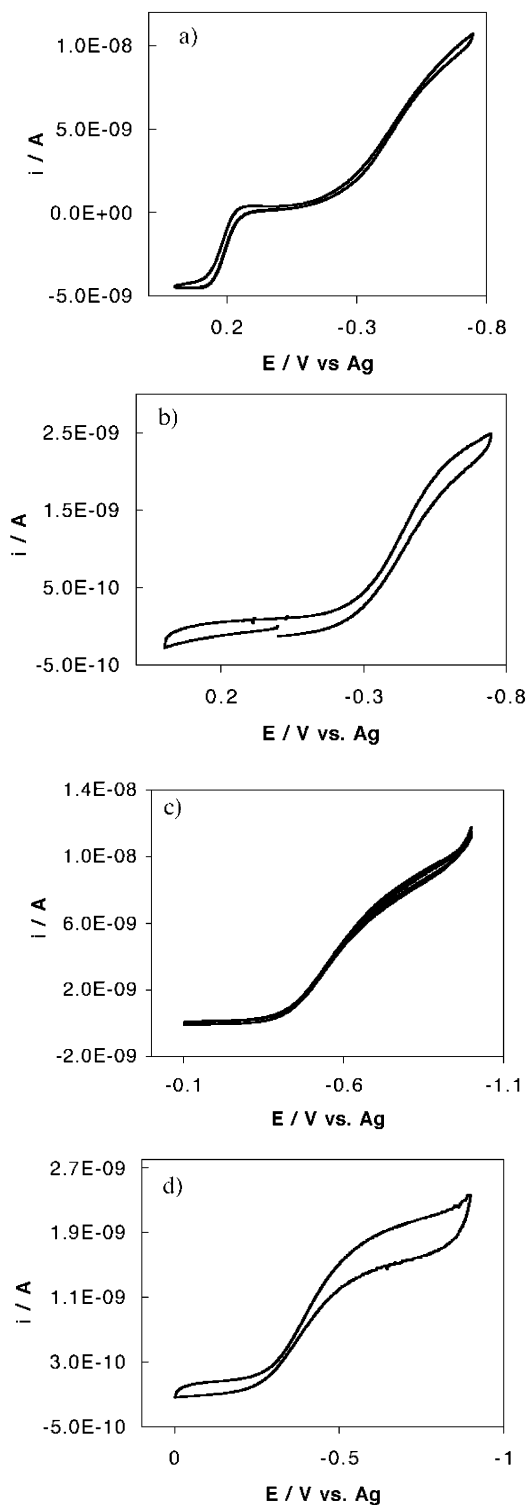
(16) Liu, B.; Bard, A. J. *J. Phys. Chem. B* **2002**, *106*, 12801.

Figure 2. (a) Cyclic voltammogram (scan rate 0.05 V s^{-1}) for bare 25-μm Pt disk, Ag ring electrode in air-saturated 1 mM ferrocenemethanol solution with 0.1 M NaCl as supporting electrolyte. (b) Cyclic voltammogram (scan rate 0.05 V s^{-1}) for membrane-covered 25-μm Pt disk, Ag ring electrode in air-saturated 1 mM ferrocenemethanol solution with 0.1 M NaCl as supporting electrolyte, with 10-μm-thick HDPE membrane. (c) Five consecutive cyclic voltammograms (scan rate 0.05 V s^{-1}) for the reduction of oxygen in air-saturated 0.1 M pH 7 PBS, at bare Pt disk, Ag ring electrode, after activation procedure described in text. (d) Cyclic voltammogram (scan rate 0.05 V s^{-1}) for the reduction of oxygen in air at 25-μm Pt disk, Ag ring electrode, with 10-μm-thick HDPE membrane and 0.1 M pH 7 PBS as electrolyte.

Figure 2b shows a CV obtained in the same ferrocenemethanol solution after the polyethylene membrane containing a drop of 0.1 M NaCl electrolyte solution had been placed over the electrode. The oxidation wave for the ferrocenemethanol is absent from this CV, providing good evidence that the membrane prevents the diffusion of solution species to the electrode surface and indicating an absence of pinholes. The reduction current for oxygen is still present but with a reduced value of the cathodic current at −0.75 V (note change of scale on the *y*-axis). This shows that oxygen can selectively diffuse through the membrane but suggests that the diffusion coefficient for oxygen through the membrane is lower than that for diffusion of oxygen through aqueous solution. These results are important for the use of this sensor in media that contain other electroactive species (especially in the liquid phase) that could interfere with oxygen measurements. The polyethylene membrane therefore ensures the selectivity of the electrode toward oxygen reduction. Again, no diffusion-limited steady-state current was obtained using 0.1 M NaCl as the electrolyte.

Figure 2c shows five consecutive CVs for oxygen reduction at the bare electrode (no membrane) in an air-saturated 0.1 M pH 7 PBS solution. The electrode was first activated by repeatedly cycling between −0.35 and 1.2 V versus Ag until reproducible CVs were obtained. The electrode was then cycled from −0.1 to −1.0 V until consistent CVs for oxygen reduction were obtained (~10 scans). The figure shows that this procedure results in very reproducible CVs for oxygen reduction. The limiting behavior of the electrode is still relatively ill defined, as the current never reaches a clear plateau. However, the region of oxygen reduction before the onset of water reduction at −0.92 V can be better distinguished using this buffered electrolyte.

The CV for oxygen reduction in the gas phase is shown in Figure 2d for the electrode equipped with a membrane containing a drop of 0.1 M pH 7 PBS electrolyte. This experiment was performed by clamping the electrode in air and scanning the potential toward negative values to −0.9 V versus Ag. As in solution, although a clear limiting plateau was not found, a region of relatively steady-state current was found from −0.65 to −0.85 V before the onset of electrolyte reduction. Multiple scans exhibited no appreciable change, and all the curves essentially overlapped. The value of limiting current obtained was relatively consistent between experiments even when the membrane and electrolyte were changed. The value of limiting current for oxygen reduction in air was always of the order of 2 nA, consistent with a diffusion coefficient for oxygen through the membrane of D_m ~ 1 × 10⁻⁷ cm² s⁻¹. The response time, τ, of the electrode is the time taken for 99% of the signal change on an alteration of oxygen concentration and can be calculated according to the following relation:[4]

$$\tau \cong 0.53 z_m{}^2 / D_m$$

where z_m is the thickness of the membrane and D_m the diffusion coefficient of the species through the membrane. For a 10-μm-thick membrane and D_m ~ 1 × 10⁻⁷ cm² s⁻¹, τ is ~5 s. This parameter is important when the electrode is used as a SECM tip and governs the maximum rate of approach (*z* direction) to the surface and the maximum scan rate (*x* and *y* directions) during
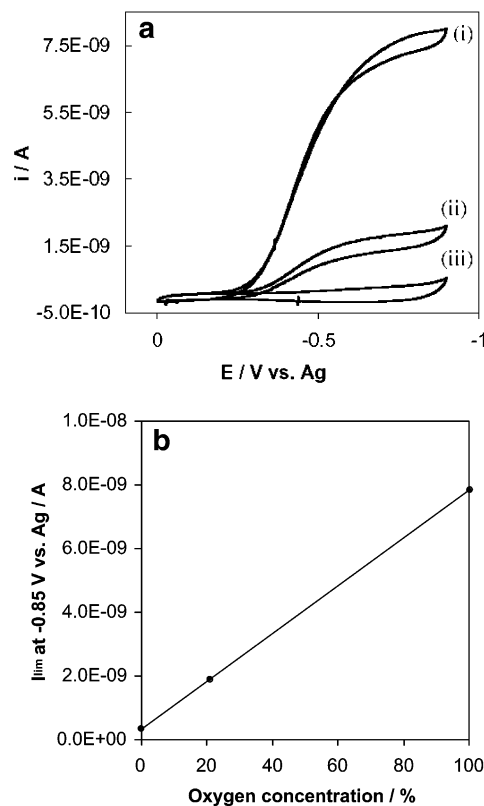

Figure 3. (a) Cyclic voltammograms (scan rate 0.05 V s⁻¹) for the reduction of oxygen at 25-μm Pt disk, Ag ring electrode, with 10-μm-thick HDPE membrane and 0.1 M pH 7 PBS as electrolyte. (i) In 100% oxygen. (ii) In air (20.9% oxygen). (iii) In argon (0% oxygen). (b) Calibration plot for the relationship between tip current at −0.85 V and gaseous oxygen concentration for a 25-μm Pt disk, Ag ring electrode, with 10-μm-thick HDPE membrane and 0.1 M pH 7 PBS as electrolyte.

imaging. In contrast, the basic UME response time without a membrane is given by $\tau \sim r^2/D_s$, where r is the radius of the electrode and would be ~70 ms.

An important property for an oxygen-sensing electrode is that a linear electrochemical response is obtained with oxygen concentration. The electrode was calibrated in the gas phase by carrying out experiments in a tube with an inlet and outlet for the flowing of gases (argon and oxygen) and an aperture for the sensor. The cyclic voltammetric response of the electrode was recorded for air, pure oxygen, and pure argon. Figure 3a shows the CVs obtained for (i) 100% oxygen, (ii) 20.9% oxygen (air), and (iii) 0% oxygen (pure argon). Figure 3b shows the limiting current for the CVs at −0.85 V versus Ag plotted against oxygen concentration. The relationship is linear, showing that the observed limiting current of the membrane-covered electrode is directly proportional to the oxygen concentration in the gas phase.

SECM Approach Curves. (A) Response of Tip to Oxygen Reduction. An approach curve is a plot of the tip current, i_T, as a function of tip−substrate separation, d, as the tip is moved from a distance several tip diameters away toward the substrate. Approach curves can provide information about the nature of the substrate and, importantly, allow the distance of the tip from the substrate surface to be determined. Ordinarily, the approach of a disk-shaped tip to within a few tip radii of an insulating surface causes a blocking of the diffusion of the reactant to the tip, and a

resulting drop in tip current occurs in a process called negative feedback. The fitting of experimentally obtained approach curves with theory allows us to gain information about the behavior of the tip, as well as accurately locate its position above a substrate.

A schematic depiction of the steady-state oxygen concentration profiles at a membrane UME is shown in Figure 4a, where x is the distance from the electrode surface. As calculated above, the diffusion coefficient for oxygen through the membrane, D_m, is $\sim 1 \times 10^{-7}$ cm^2 s^{-1}. Comparison of this value with that for diffusion of oxygen to the membrane in air, $D_a \sim 0.2$ cm^2 s^{-1}, and diffusion of oxygen in solution, $D_s \sim 2 \times 10^{-5}$ cm^2 s^{-1}, shows that the magnitude of the current for oxygen reduction is limited by the rate of diffusion of oxygen through the membrane. The current is therefore governed by the diffusion through the membrane (thickness, $b - a$) and internal electrolyte layer (thickness, a), and its magnitude, i, is given by

$$\frac{i}{nF} = \frac{D_m(C_b - C_a)}{(b - a)} = \frac{D_s C_a}{a} \tag{1}$$

where n is the number of electrons in the reaction ($n = 4$ for oxygen reduction at Pt) and

$$C_a = \xi C_b / (1 + \xi) \tag{2}$$

where

$$\xi = \frac{D_m}{D_s}\left(\frac{a}{(b - a)}\right) \tag{3}$$

under conditions where $D_m \ll D_s$ and $a \approx (b - a)$, $C_a \approx \xi C_b$. In many applications of membrane electrodes, C_b is close to the value of the bulk concentration of oxygen, C^* (assuming no preferential distribution of oxygen into the membrane), so the current is proportional to the concentration of oxygen incident at the membrane surface. Therefore, for SECM approach curves, when the tip (of radius r) is brought near to an insulating substrate, oxygen depletion in the gap $c - b$ (where $(c - b) < 5r$), by the reaction at the membrane surface and blocked diffusion of fresh oxygen, should cause a decrease in the current. From the SECM theory for insulating substrates,[14] the plot of the normalized tip current, $i_T/i_{T,\infty}$, with normalized distance, $L = d/r = (c - b)/r$, should be independent of the diffusion coefficient, so the same approach curve should be found in the gas phase and in solution.

For this membrane-covered UME containing 0.1 M pH 7 PBS electrolyte, approach curves to a nonconducting (glass) surface were obtained in both solution and gas (air) phases. Figure 4b shows an experimental approach curve of the UME without a membrane to an insulating surface in air-saturated 0.1 M pH 7 PBS, at an approach rate of 1 μm s^{-1} (solid line) and a tip potential of -0.85 V, along with the theoretical approach curve calculated for this system (gray line). The figure shows that the UME behaves as a typical SECM tip when employed for oxygen reduction without a membrane in solution, and the approach curve agrees very well with the theoretical one.

Figure 4c shows an approach curve (solid line) obtained at a tip potential of -0.85 V for the same UME in solution, but with a
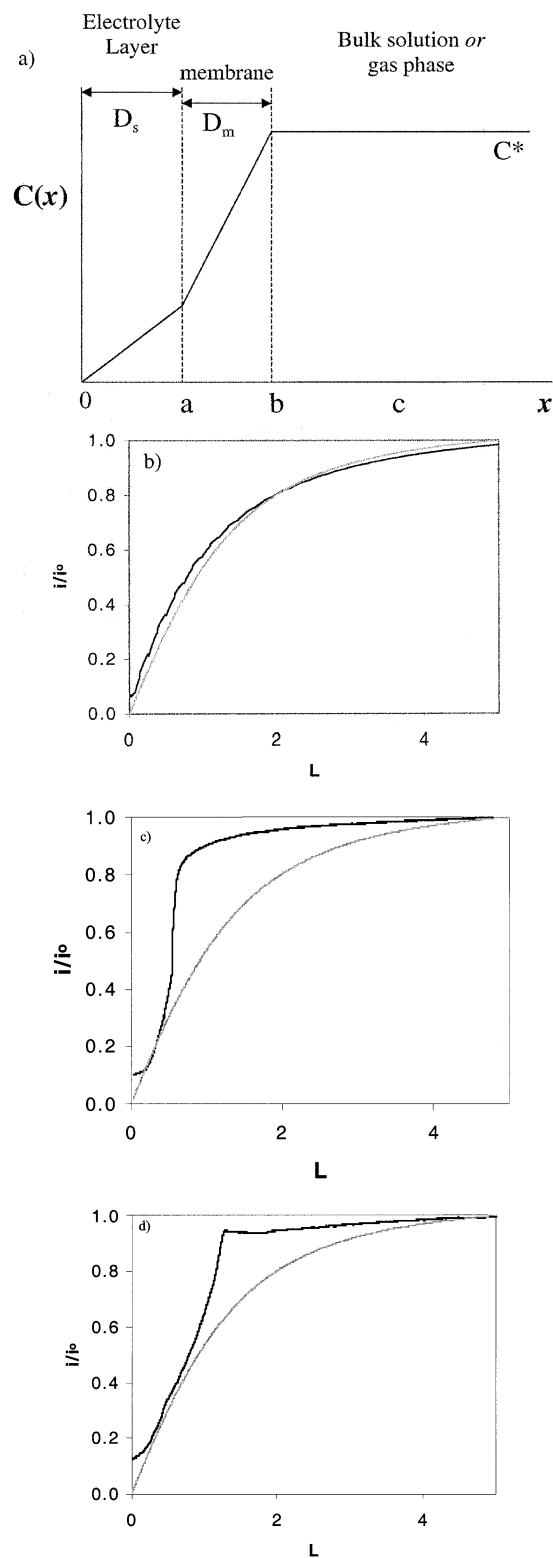

Figure 4. (a) Schematic diagram of limiting steady-state concentration profiles of oxygen, $C(x)$ is the concentration of oxygen, and x is the distance from electrode at the membrane UME. Experimental (solid line) approach curves (approach rate 1 μm s^{-1}) for 25-μm Pt disk, Ag ring electrode to insulating (glass) surface with theoretical curve (gray line) for oxygen reduction at -0.85 V vs Ag. Currents normalized to limiting current at infinity (i_∞) and with $L = d/r$, where d is the distance from tip to substrate and r is the radius of the tip. (b) Bare electrode in air-saturated 0.1 M pH 7 PBS. (c) Electrode with HDPE membrane with 0.1 M pH 7 PBS electrolyte in air-saturated water. (d) Electrode with HDPE membrane with 0.1 M pH 7 PBS electrolyte in air.

membrane. This curve deviates markedly from theory (gray line) and shows considerably less negative feedback than predicted at distances $L > 0.5$. The drop in current with distance to the substrate is much less gradual than observed in the absence of a membrane, with a sharp drop in current at distances very close to the insulating surface.

Figure 4d shows the same experiment repeated in air (solid line) at an approach speed of 1 μm s^{-1} along with the theoretical curve (gray line). The approach curve in the gas phase is similar to that in solution with a membrane and shows a much less gradual drop in normalized tip current with distance than predicted. In other words, the steady-state current does not begin to drop until distances much closer to the electrode, even at a very slow approach rates down to 0.01 μm s^{-1}.

Three considerations in SECM approach curves with an oxygen membrane electrode are (1) the longer response time due to the membrane, (2) deactivation of the Pt, and (3) the presence of convection in the gas phase. The deactivation problems of Pt can be overcome, as discussed previously, by suitable electrode pretreatment or by the application of a potential program to the tip. The two factors causing deviation from theoretical behavior are, therefore, likely to be the increased response time of the tip from 70 ms to 5 s on application of a membrane and the rapid diffusion and presence of convection in the gas phase.

In the gas phase, the low viscosity of the air means that small drafts and density gradients (e.g., created by thermal gradients) can cause convective flow and erase diffusion layers. Greatly reduced (less steep) concentration gradients in the air phase due to fast diffusion of oxygen in air coupled with slow diffusion in the membrane leads to less well defined diffusion layers that are readily perturbed by convective flow. Moreover, the movement of the z scanner itself during approach could cause convection. For these reasons, the behavior of the electrode in the gas phase cannot be modeled using equations derived from assumptions in the solution phase.

In addition, theoretically the form of the current−distance approach curve should be independent of diffusion coefficient; however, the large value of the diffusion coefficient for oxygen in air ($D_a = 0.2$ cm^2 s^{-1}) in comparison with that in solution ($D_s = 2 \times 10^{-5}$ cm^2 s^{-1}) may lead to a breakdown in the usual SECM model. For example, in solution under usual SECM conditions, diffusion of electroactive species from above the plane of the insulated disk tip makes a negligible contribution to the flux and current. This will not be so when the diffusion coefficient is very large. In the gas phase, the large magnitude of the diffusion coefficients (as well as convection) means that a clear diffusion layer will never be established so that the theory derived by the solution of diffusion equations, such as that for approach of a tip to an insulting surface, is less useful in the gas phase.

To investigate the effect of convection on approach curves obtained in the gas phase, an experiment was performed where amperometric current versus time curves (at applied potential −0.85 V) were recorded at different distances from the insulating surface. This technique allows time for the concentration of oxygen at the electrode to equilibrate, which compensates for the increased response time, and should also eliminate any undesired convection due to the motion of the tip toward the insulating surface. The limiting current values after 60 s for each i−t curve
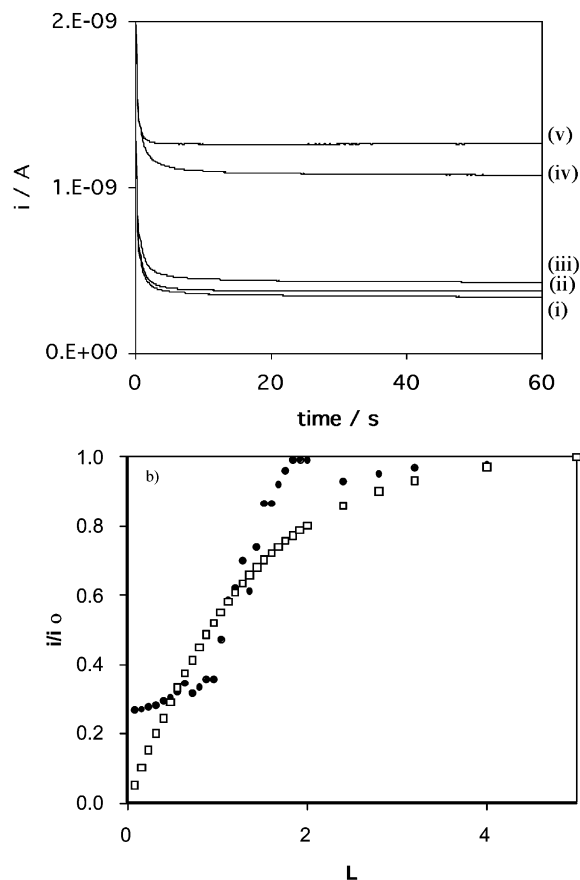

Figure 5. (a) Chronoamperometric (current−time) curves for membrane 25-μm Pt UME at distances of (i) 0, (ii) 5, (iii) 10, (iv) 20, and (v) 100 μm from an insulating surface in air. Applied potential −0.85 V vs Ag. (b) Approach curve derived from plot of normalized limiting current from current−time curves after 60 s versus normalized distance from insulating surface in air (black circles). With theoretical approach curve to insulating surface (open squares).

were plotted versus the distance from the surface at which the curve was acquired and the resulting plot mathematically treated as an approach curve. Figure 5a shows some representative i−t curves obtained at different distances from the surface for this experiment, and Figure 5b shows the plot of the limiting currents after 60 s with distance from the insulating surface. As can be seen in Figure 5b, the approach curve derived by using this technique (black circles) deviates a little less from theory (open squares) than that of Figure 4d acquired in air with the standard procedure. The shape of the curve is still not as smooth as expected, and this is probably due to stray diffusive/convective effects that are not eliminated by the technique. This figure shows that convection is a contributing factor to the form of the approach curve found for oxygen reduction in the gas phase.

Although convection may justify why deviations from theory are found in the gas phase, the form of the approach curve obtained in Figure 4c for the membrane UME in solution cannot be explained in this manner. In this case, the lack of negative feedback may be attributed to the long response time of the electrode for the detection of oxygen (5 s). The speed of tip approach to the surface (1 μm s^{-1}) does not allow sufficient time for the electrode to react to the decrease in oxygen concentration in the negative feedback region. In Figure 4d in the gas phase, where the lack of negative feedback is still more severe, the
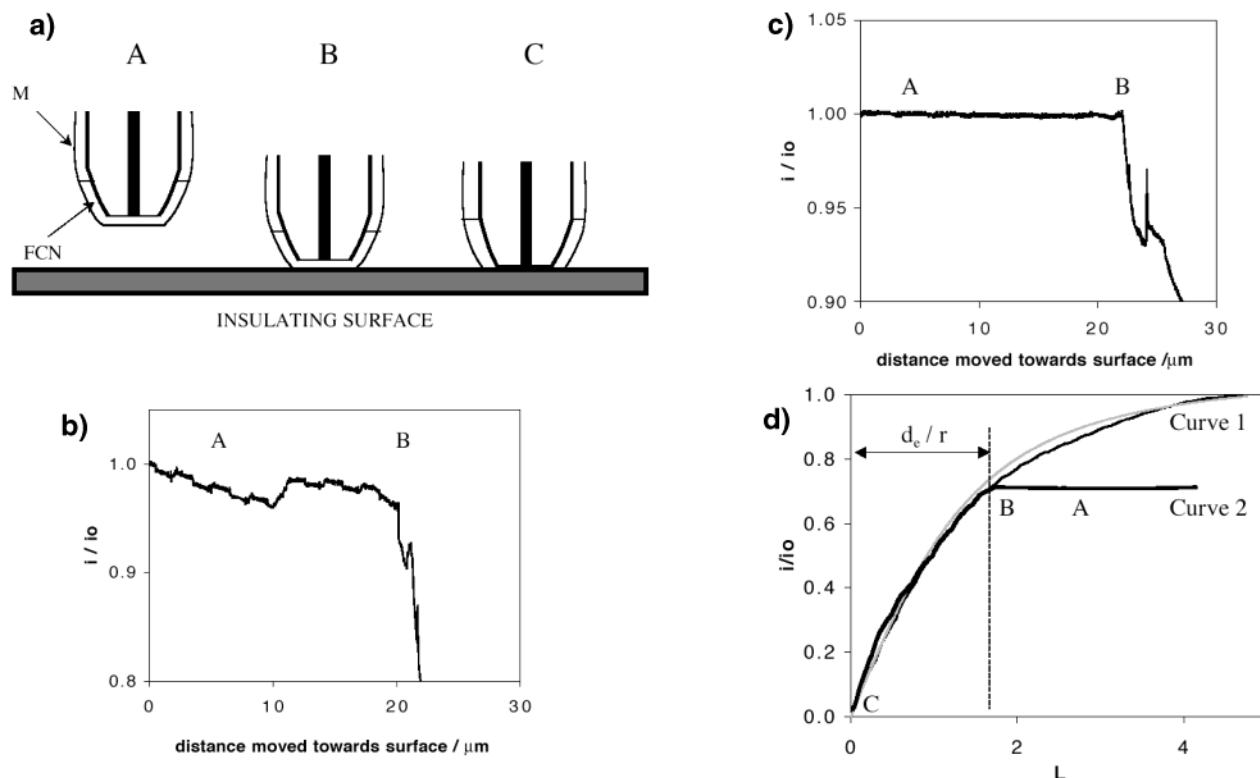
Figure 6. (a) Schematic of processes occurring as membrane UME, containing 1 mM ferrocenemethanol as electrolyte, approaches an insulating surface. (A) electrode is far from the surface; (B) membrane touches the surface; (C) tip touches the surface, electrolyte layer is squashed between electrode surface and membrane. FCN, ferrocenemethanol electrolyte layer; M, membrane. (b) Experimental approach curve (approach rate 1 μm s^{-1}) starting ~20 μm above an insulating surface for membrane 25-μm Pt UME, with 1 mM ferrocenemethanol (in 0.1 M NaCl) as electrolyte, with tip potential +0.4 V vs Ag. Current normalized to limiting current at infinity (i_∞); (A) and (B) correspond to conditions A and B in (a) above. (c) Experimental approach curve (approach rate 1 μm s^{-1}) starting ~20 μm above an insulating surface for membrane 25-μm Pt UME, with 1 mM ferrocenemethanol (in 0.1 M NaCl) as electrolyte, with tip potential −0.85 V vs Ag for oxygen reduction. Current normalized to limiting current at infinity (i_∞); (A) and (B) correspond to conditions A and B in (a) above. (d) Curve 1: first approach curve (approach rate 1μm s^{-1}) to an insulating surface for membrane 25-μm Pt UME, with 1 mM ferrocenemethanol (in 0.1 M NaCl) as electrolyte, with tip potential +0.4 V vs Ag. Curve 2: second approach of membrane UME to insulating surface after withdrawal of 100 μm from surface after curve 1. Currents normalized to limiting current at infinity (i_∞) and with $L = d/r$, where d is the distance from tip to substrate and r is the radius of the electrode. (A−C) correspond to positions A−C in (a); d_e is the thickness of the electrolyte layer.

deviation from theory is likely due to a combination of convection, high diffusion coefficient, and increased response time.

The above discussion does not explain why such a severe decrease in tip current is obtained at all, if negative feedback cannot be readily detected by this system. The sudden drop in current could be attributed instead to the compression of the electrolyte layer between the membrane and the electrode surface as the membrane contacts the substrate. This effectively physically blocks oxygen from diffusing through the membrane to the electrode surface, and the resulting tip current is then due exclusively to the oxygen already dissolved in the inner-membrane electrolyte layer. As the electrolyte layer is further compressed, the electrode experiences negative feedback for oxygen reduction in the electrolyte, which explains the dramatic drop in tip current. Eventually, the current tends to zero as the electrolyte layer thickness is reduced to an extent that electrical contact is lost between the Pt cathode and Ag anode.

This has been explored further by looking at the approach curves of the membrane UME using 1 mM ferrocenemethanol in 0.1 M NaCl as the electrolyte layer between the membrane and the tip. In the first experiment, an approach curve to an insulating surface in air was recorded using an applied voltage of 0.4 V versus Ag. The tip current recorded over distance was,

therefore, that for the oxidation of the ferrocenemethanol in the electrolyte layer inside the membrane. Figure 6b shows part of the resulting experimental approach curve taken at a scan rate of 1 μm s^{-1}. The x axis shows the absolute distance moved by the tip *toward* the surface during the experiment, rather than the distance *from* the surface. The current, although noisy, remains essentially constant until the membrane touches the substrate surface at ~21 μm and then the electrolyte layer begins to be squashed between the substrate surface and the tip. The current falls rapidly as the electrolyte layer becomes thinner and diffusion of ferrocenemethanol to the electrode surface is blocked (negative feedback region). Figure 6a shows a schematic of the process taking place during the approach to the surface. Initially, the electrode is far from the surface as shown in (A) and the current is at a steady-state value, but at point B the membrane touches the surface and the electrolyte layer begins to be squashed between the tip and the substrate. At point C, the tip itself has touched the membrane and there is no electrolyte layer remaining between the electrode and the membrane so the current is essentially zero. The parts of the approach curve in Figure 6b corresponding to processes A and B are labeled.

In a second experiment, the electrode was withdrawn from the surface to the same distance as the first approach was started

and the approach curve repeated, but with the potential held at − 0.85 V for oxygen reduction. Figure 6c shows the resulting approach curve. This curve has the same form as that for ferrocenemethanol, with the rapid drop of current at ∼22 μm corresponding to the point at which the membrane first touches the surface. This clearly illustrates that negative feedback is not observed for oxygen reduction in the gas phase, and the dramatic drop in current in Figure 4d at $L = 1$ can be attributed to the contact of the membrane with the substrate surface and the resulting deformation of the electrolyte layer. Note that when the membrane is in contact with the surface, the tip current for oxygen reduction is also sensitive to the surface topography of the substrate, which must be taken into account during imaging applications.

(B) Determination of Electrolyte Layer Thickness inside the Membrane. As described above, when ferrocenemethanol is used as the electrolyte solution inside the membrane, the current obtained at the oxidation potential of −0.4 V is strongly influenced by the thickness of the electrolyte layer. When an approach curve is recorded for the membrane UME approaching an insulating surface, the current for the oxidation of ferrocenemethanol begins to decrease after the membrane has come into contact with the surface. This is because the electrolyte layer thickness between the membrane and the tip decreases as the electrode tip moves closer to the membrane and the solution is displaced from this region to around the glass sheath of the electrode within the membrane. The approach of the tip toward the membrane in this regime can be compared to the approach of a tip in solution toward an insulating substrate and the resulting decrease in oxidation current is due to negative feedback, as the diffusion of fresh ferrocenemethanol to the tip surface is blocked. The measurement of approach curves using ferrocenemethanol as an electrolyte and the oxidation potential 0.4 V allows an estimate of the thickness of the electrolyte layer. In this case, we are measuring the current response for the oxidation of the ferrocenemethanol inside the membrane, and this will change as a function of electrolyte layer thickness, as described above. From the theory for the approach of a tip to an insulating substrate (in this case the membrane), a tip with a 12.5-μm radius will begin to experience negative feedback at an electrolyte layer thickness of less than ∼60 μm ($L = 5$).

Figure 6d shows such a case in curve 1, where the response of the tip current as the tip approaches the membrane corresponds almost exactly to that predicted from theory (gray line). For this membrane UME, the electrolyte thickness can be estimated as at least 60 μm. After withdrawing the electrode and approaching the surface again, a different approach curve was obtained, as shown in curve 2 of Figure 6d. This time, the electrolyte layer has been squashed during the previous approach to the surface in curve 1, so it started out thinner than the previous one. This means that the electrode is already within the negative feedback region and the value of the constant current obtained initially reflects this, as it corresponds to a value of ∼0.7 i/i_∞ on the first approach curve. At this point, the membrane has not touched the surface, corresponding to position A in Figure 6a. The current begins to drop only when the membrane touches the insulating surface (position B) at $L = 1.68$ and the electrolyte begins to be squashed between the membrane and the tip. Thereafter, the
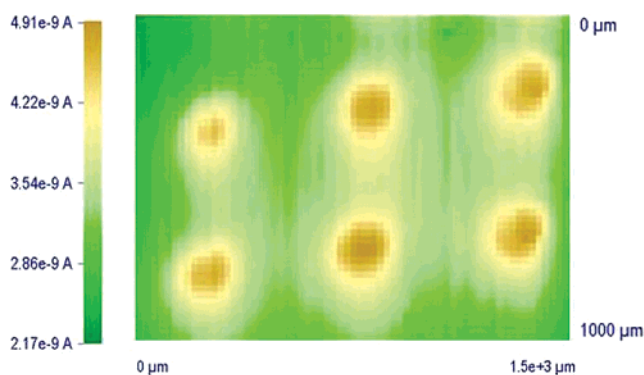
Figure 7. SECM image obtained in the gas phase by scanning the membrane 25-μm Pt UME in the $x−y$ plane ∼10 μm above an array of six 100 μm × 100 μm holes spaced 400 μm apart in a silicon wafer with pure oxygen flowing through the holes. Tip potential −0.85 V vs Ag; scan speed 1 μm s^{-1}.

electrode experiences negative feedback as the diffusion of fresh ferrocenemethanol is blocked. The drop in current can be fit to the theory for negative feedback between point B, when the membrane first touches the surface, and point C, when the tip touches the membrane and the electrolyte layer is reduced to near zero, as shown in Figure 5d. This allows an estimate of the electrolyte layer thickness as $L = 1.68$, which corresponds to d_e = 21 μm. The results in Figure 6d therefore show that the thickness of the electrolyte layer varies from 60 to 20 μm depending on how the membrane is constructed and whether it has already been used to approach and contact a surface. Note that this concept of employing an electroactive species in the electrolyte layer can be useful in monitoring this layer thickness.

SECM Imaging of the Oxygen Flux at a Silicon Wafer Array. To demonstrate the imaging capability of this oxygen sensor as a SECM tip, we used a silicon wafer through which six holes of 100-μm diameter were drilled, spaced 400 μm apart in a 2 × 3 array. The array was taped to a Teflon support on the SECM stage in air, and a flow of oxygen gas was introduced from below in order to create a flux through the holes.

First, an approach curve was obtained for the membrane UME tip at −0.85 V in air, approaching the silicon surface at a position far from the holes and in the absence of an oxygen flux through the holes to obtain a negative feedback approach curve, similar to that in Figure 4d. The distance at which the current experiences a sharp decrease enables the determination of the point at which the membrane touches the surface, as discussed above. The tip was then withdrawn so that the membrane was about 10−20 μm above the surface. At this distance above the surface, the electrode was scanned (speed 1 μm s^{-1}) in the $x−y$ plane above the six holes, with the potential held at −0.85 V and oxygen gas flowing through the apertures. As the tip current is directly proportional to oxygen concentration (Figure 3), a plot of the current versus scanned area allows us to obtain an image of the regions of greater oxygen flux. The image obtained is shown in Figure 7 and clearly shows the six areas of increased tip current corresponding in position and dimension to the holes in the silicon array. The same scan performed in the absence of an oxygen flux showed a constant tip current over the same area and did not allow features to be distinguished.

The distance of the tip from the substrate is an important factor, since it greatly affects the quality of the image and the quantitative

information that can be deduced. If the membrane is too close to the surface and touching, the tip current will vary with electrolyte thickness and will depend on the topography of the substrate rather than detecting oxygen concentration in the gas phase. However, if the electrode is too far from the surface, resolution of the size and morphology of the holes will be poorer, due to diffusion of the oxygen as it emerges through the holes.

CONCLUSIONS

A Clark-type sensor for oxygen, based on a 25-μm platinum tip, was characterized and used as a probe for scanning electrochemical microscopy in the gas phase. The sensor was assembled using a conventional ultramicroelectrode covered with a HDPE membrane. Electrochemical measurements demonstrated that stability of the probe in the measurement of the oxygen reduction signal could be achieved by using a suitable electrolyte (pH 7 PBS) and a program of electrode activation. The membrane integrity that provides selectivity for the system and confinement of the electrolytic solution can be checked for pinholes by performing cyclic voltammetry in an external solution containing a redox couple. The tip current at -0.85 V shows a linear relationship with oxygen concentration.

Experimental SECM approach curves for the membrane UME deviate from those expected from theory due mainly to the increase in response time of the electrode to 5 s on application of a membrane. The theory for the approach of an electrode to an insulating substance assumes that tip current will be independent of diffusion coefficient, but this may not be true for the large diffusion coefficients observed in the gas phase. In this case, approach curves may be interpreted in terms of the membrane touching the surface and in this way allow the distance of the tip from the inner surface of the membrane to be determined. The use of ferrocenemethanol as the electrolyte within the membrane allows a determination of the thickness of the electrolyte layer as $20-60$ μm. The use of SECM in the imaging mode allowed the flux of oxygen through an array of holes of 100-μm diameter to be imaged.

For imaging applications requiring greater resolution, the problem of the undesirably long response time of the UME will need to be addressed. To increase the response time, it will be necessary to decrease the thickness of the membrane or use a membrane material more permeable to oxygen.